BIOMETRICAL APPROACHES FOR MANDARIN LEAF IMAGE ANALYSIS

J. KRISTON-VIZI[1]* – A. FERENCZY[2] – M. UMEDA[3] – K. MIYAMOTO[4]
*e-mail: kriston@omega.kee.hu

[1] Budapest University of Economic Sciences and Public Administration,
Faculty of Horticultural Sciences, Technical Department
H-1118 Budapest, Villányi út 31.
(phone: +36-1-372-6265)
[2] Budapest University of Economic Sciences and Public Administration,
Faculty of Horticultural Sciences, Department of Mathematics and Informatics,
H-1118 Budapest, Villányi út 31.
[3] Laboratory of Field Robotics, Division of Environmental Science and Technology,
Graduate School of Agriculture, Kyoto University, Japan
[4] Wakayama Research Center of Agriculture, Forestry and Fisheries,
Arida-gun Wakayama, Japan

(Received 5th Jan 2004; accepted 10th May 2004)

Abstract. A study examining correlations between fruit trees physiological and visual properties collected by remote sensing technology started at Budapest University of Economic Sciences and Public Administration, Faculty of Horticultural Science, together with Kyoto University and Wakayama Research Center of Agriculture, Forestry and Fisheries, Fruit Tree Experiment Station (Japan). Experimental plant was Satsuma mandarin (*Citrus unshiu* MARC. var. satsuma), the physiological property to examine was leaf water potential, which correlates with the sugar content of mandarin fruit according to preceding studies. Large amount of visual information had been recorded at ground level and was processed by the methods of image analysis and biometry. Under field conditions images of given leaves showed different type of reflectance frequency distribution. These distributions often could be identified as normal distribution, however left skewed, right skewed and bimodal distributions also occurred even partially shifted out of the perceptive range of the measuring device. Comparison of the applied biometric methods was analyzed to adjust with the natural field conditions, hardware and software features.
Results showed that normal distribution model could be applied for analyzing data obtained at optimal conditions, however these phenomena under natural field conditions could often be described better when weighted averaging methods were applied on frequency distributions.
Keywords: *image analysis, satsumas, mandarin, multispectral, NDVI*

Introduction

A study began at Budapest University of Economic Sciences and Public Administration Faculty of Horticultural Sciences (former SZIU Faculty of Horticultural Sciences) together with Kyoto University and Wakayama Research Center of Agriculture, Forestry and Fisheries, Fruit Tree Experiment Station (Japan) on examining the correlation between fruit tree physiological and visual properties collected by remote sensing technology.

http://www.ecology.kee.hu • ISSN 1589 1623

Like most taxons, drought stress effects many plant physiological properties of citruses including photosynthesis [1], sugar accumulation [2, 3] fruit growth [4], stomatal closure [5] and abscisic acid content [6].

Experimental plant was Satsuma mandarin (*Citrus unshiu* MARC. var. satsuma), the examined physiological property was leaf water potential, which is correlated to the sugar content of mandarin fruit in peel, locular membrane, and juice sac [7]. Related to the topic, Láng et al. [8, 9, 10] conducted successful researches to reveal correlations between fruit tree leaf color spectra and nutrition supply. Working on „Aoshima" Satsuma mandarin, Iwagaki [11] reported higher sugar content, improved rind color, ans increased citric acid content.

'Field spectroscopy' term was introduced in 1974 by Longshaw [12] and its usage is supported by several researchers. As Milton writes: "Field spectroscopy involves the study of the interrelationships between the spectral characteristics of objects and their biophysical attributes in field environment" [13]. In this case spectral characteristics mean reflectance at some spectral channels, and objects mean individual leaves or full canopy of either one tree or a whole orchard. A simpler method of measuring the above mentioned objects' reflectance is to compare the radiance of those objects to that of the radiance of a portable reflectance target having known characteristics. Palmer [14] lists desired characteristics of such a reference target, and suggests the Kodak Gray Card (previously also called as Kodak Neutral Card) to be the standard reflectance target. Milton [15] evaluated spectral reflectances of Kodak Gray Card over the range 400-1100 nm. His results show good consistency between cards selected from a single batch.

The method of visual data collection and numerical data extraction had already been developed [16]. Large amount of obtained data was analyzed by statistical methods, in a way to be possible to interpret by optics, image analysis, and plant production.

Objective

Fruit leaf objects were investigated by image analysis, remote sensing and field spectroscopy methods resulting frequency tables. Analyzing frequency tables, a suitable data calculation method became necessary to reduce reflectance information into a single value. Biometrical analysis seemed to be difficult, because the type of objects' empirical density function was not uniform. Development of a uniform, algorithmizable statistical method was required to be able to analyze several thousand frames (images) that showed several different distribution types.

Materials and methods

Hardware and software tools

For image recording, "Silvacam" digital false color 3 channel CCD video camera was used, made by VTT. This camera was built on JVC GY-DV500 body and was equipped with DV output. For image analysis the Aphelion software package was used made by Acdis SA and AAI Inc. Data was analyzed statistically with SPSS for Windows 10.0 Server version software package, which is the property of SPSS Inc.

http://www.ecology.kee.hu • ISSN 1589 1623

Table 1. Silvacam videocamera Spectral Channel Perceptional Specifications.

Color Channel Name on Digital Output	Spectral Channel Wavelength Range (nm)	Spectral Channel Name
Red (R)	760-900	NIR
Green (G)	580-680	Red
Blue (B)	490-580	Green

Reference objects

For calibration purpose two kind of reference objects were used.

- Kodak Gray Card (hereafter: GC as Gray Card) with known characteristics,
- a specially made calibration paper with 4 different grayscale level plates (hereafter: CP as Calibration Paper) characteristics measured by GC. (*Figure 1*)

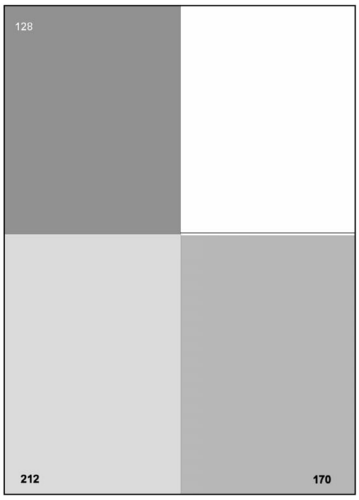

Figure 1. *Image of Calibration Paper with 4 different grayscale level plates.*

CP specifications:

- Paper material: Recycled Paper G70 A4 size, made by Toppan Forms Co. Ltd., Japan.
- Printer: Hewlett-Packard LaserJet 5000 Series PCL 6 was used to print the gray rectangle plates 212, 170, 128. The panel 255 was the pure paper surface.

Image layout

Image composition requires consideration of many factors. At first, flat field must be set to include foreground objects: leaf and reference plate. It is practical to adjust videocamera zoom setting to get the greatest virtual size of these objects on flat field, thereby maximizing objects' pixel number. During the research process image composition method had been improved empirically. The process is shown on *Figure 2-4*, as NIR channel image components in favor of higher contrast.

http://www.ecology.kee.hu • ISSN 1589 1623

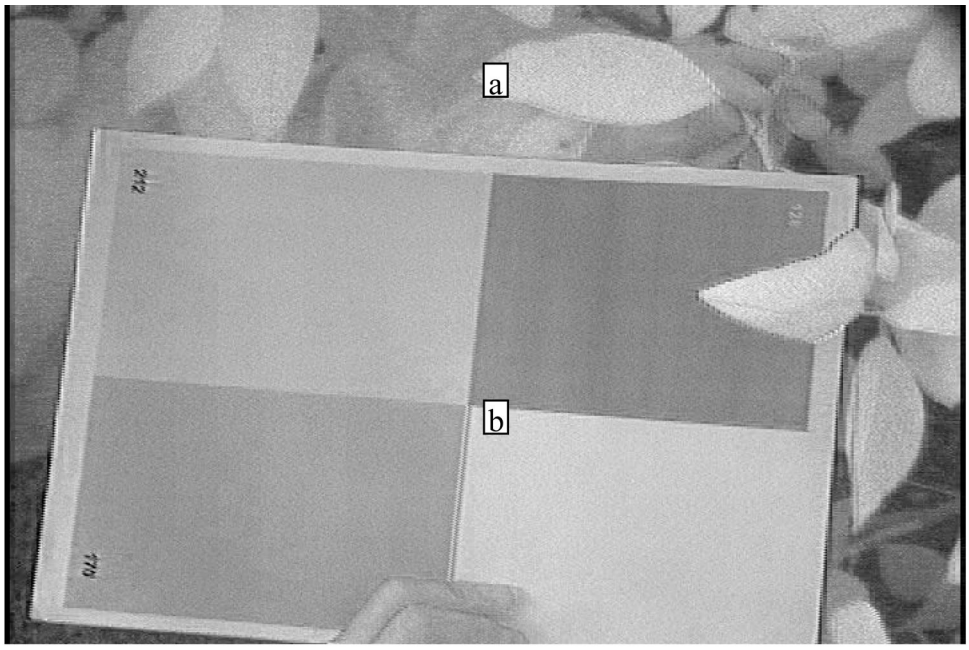

Figure 2. *Initial layout, November 2002.: leaf object to measure (a) and CP (b).*

Figure 2 shows initial layout, where most part of the flat field is covered by CP to record all 4 calibration plates, which ensures the absolute reflectance calibration in case of over- or under exposition. Due to this, image size, and pixel number of the leaf to measure is relatively small.

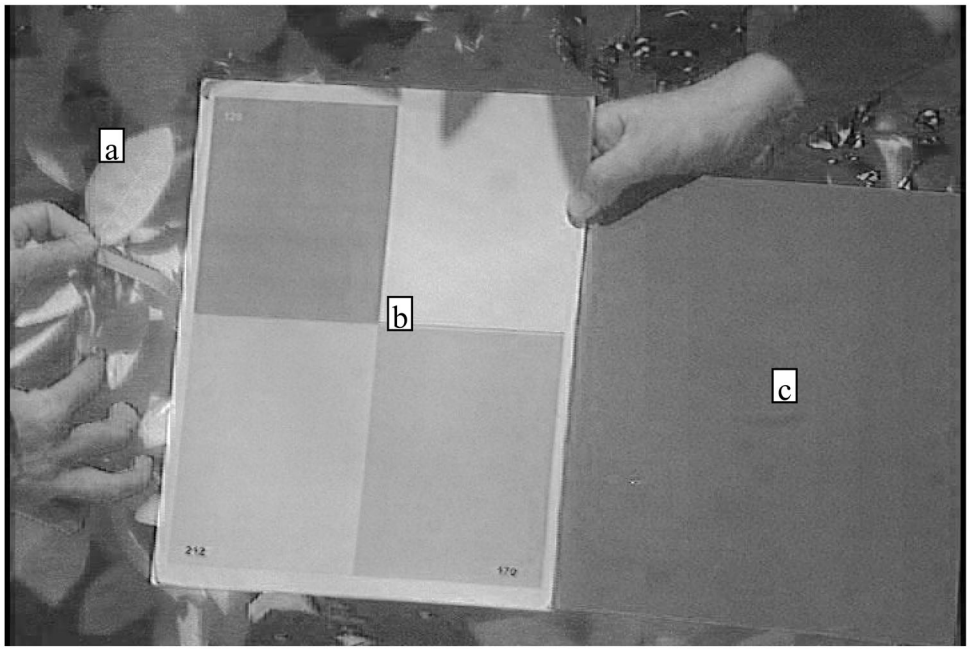

Figure 3. *August 2003.: leaf to measure (a), CP (b), GC (c).*

http://www.ecology.kee.hu • ISSN 1589 1623

On *Figure 3* CP and GC are represented together to provide maximum possibility to a successful calibration, however leaf image size became even smaller.

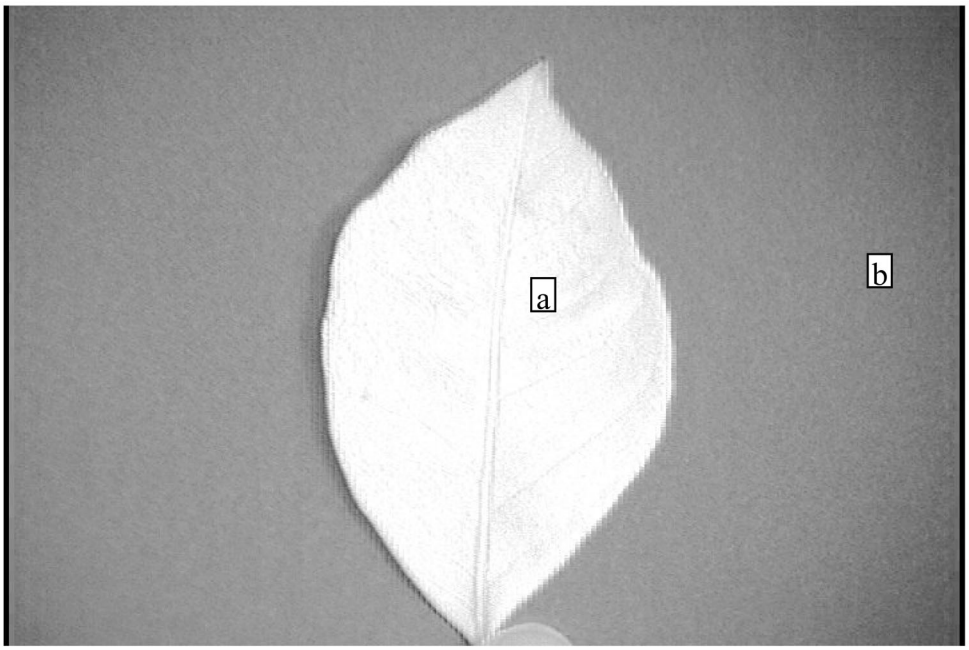

Figure 4. *December 2003.: Based on previous experiences this layout was found to be the most optimal with leaf to measure (a) and GC (b) also used as a high contrast background.*

Figure 4 depicts the most optimal image composition, that was developed by the previous experiences. Only two necessary objects are on the picture with maximal pixel numbers. This layout also gives the advantage that GC forms a high contrast background behind the leaf to determine exact leaf contour easily. In the image corners darkening, so-termed 'vignetting' effect appears.

During recording CP or GC must be exposed the same illumination conditions as the leaf to measure. Furthermore, objects must be oriented the way to avoid shadows on them, brightly colored objects reflecting light on them, and glaring (specular) reflections on objects themselves. *Figure 5* shows the optimal GC setup in daylight or artificial light.

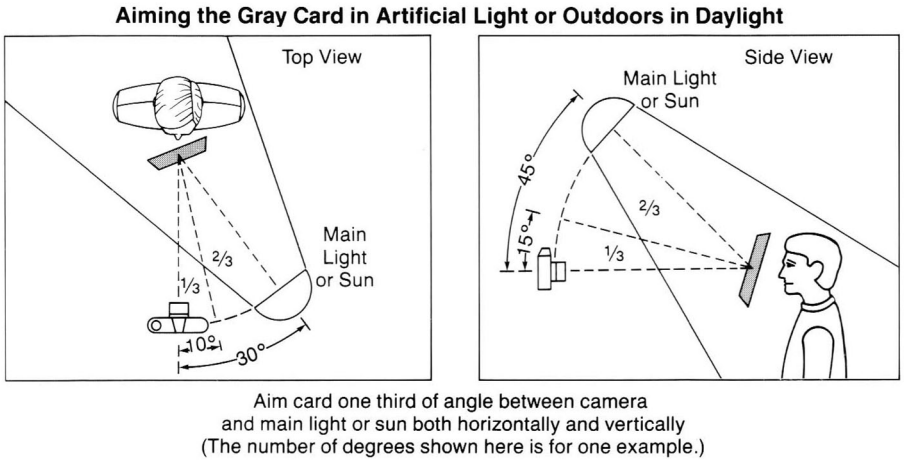

Figure 5. *GC optimal setup towards a main light source. [17]*

http://www.ecology.kee.hu • ISSN 1589 1623

Image Analysis Scheme

1. Digital Video (DV) tape was played by Silvacam videocamera and DV data stream was transferred electronically via IEEE 1394 (firewire) port to the PC's hard disk. File specifications:

1.1. uncompressed Microsoft AVI file,

1.2. Field order A,

1.3. NTSC drop frame (29.97 fps),

1.4. 720 x 480 pixel resolution,

1.5. DV Video Encoder Type 1.

2. Type 1 AVI file was converted into Type 2 AVI file.

3. Frames were extracted from Type 2 AVI file into bitmap (BMP) file. File specifications:

3.1. compression: none,

3.2. color depth: 24 bits per pixel (RGB).

4. The RGB bitmap file was splitted into 3 grayscale channels representing NIR, Red, Green spectral channels.

5. All greyscale images were segmented and numerical information was extracted into frequency tables.

Segmentation workflow

Definition of the segmentation area's outline

In the course of the image analysis the foreground area – that contains valuable information – must be separated from the background area, that does not contain valuable information from the aspect of the research aim.

In present case leaf and reference object pixels were considered as foreground information. Universal segmentation method does not exist, the given task determines how to combine and customize known segmentation algorithms to get an optimal result. Aphelion image analysis software package contains several built-in threshold-based segmentation operators for this procedure.

Threshold-based segmentation operators

Threshold-based segmentation operators are algorithms with a greyscale image as an input image and a binary image as an output image.

`AphImgThreshold` operator demonstrates the operation method of these algorithms. This operator computes a binary image using the greyscale input image, low and high threshold values as parameters. It's syntax:

$$If\ (Inimg(i,j) \geq loThresh\ \&\ \&Inimg(i,j) \leq hiThresh,\ Then\ Outimg(i,j) = 1\ else\ Outimg(i,j) = 0$$

where:

Inimg : input image

Outimg : output image

loThresh : low threshold value

hiThresh : high threshold value

In case of a high contrast image (*Figure 6*), good segmentation efficiency can be resulted, however low contrast image shows less definite result (*Figure 7*).

http://www.ecology.kee.hu • ISSN 1589 1623

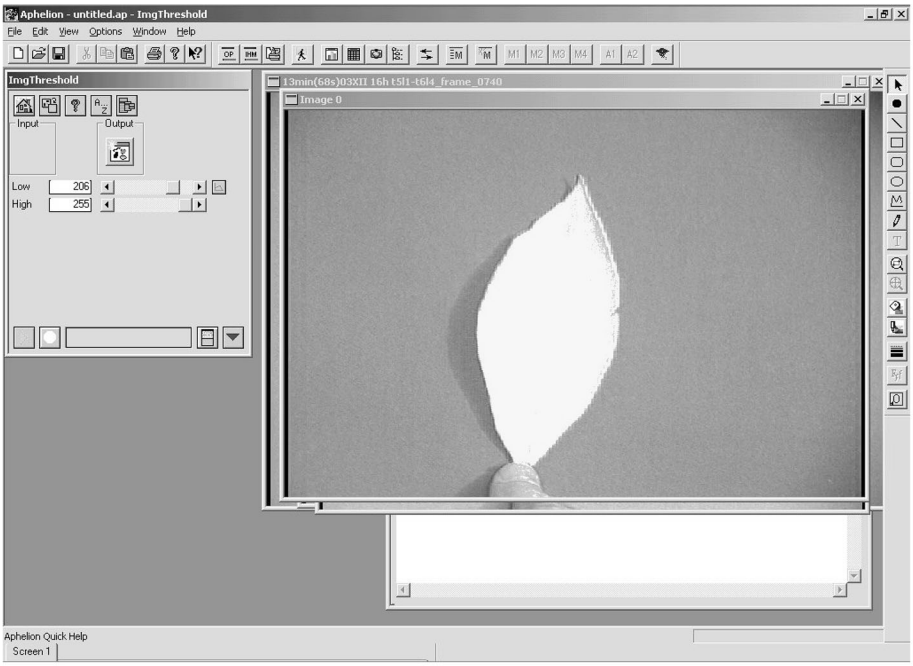

Figure 6. *Segmentation with ImgThreshold operator on a high contrast image.*

On these screenshots, fields labeled 'Low' (loThresh) and 'High' (hiThresh) indicates low and high threshold values. Segmented pixels are marked with pink color. In both cases threshold values must have been determined manually, and separately for each frames. This functional shortcoming disabled AphImgThreshold operator usage in an automatized segmentation script.

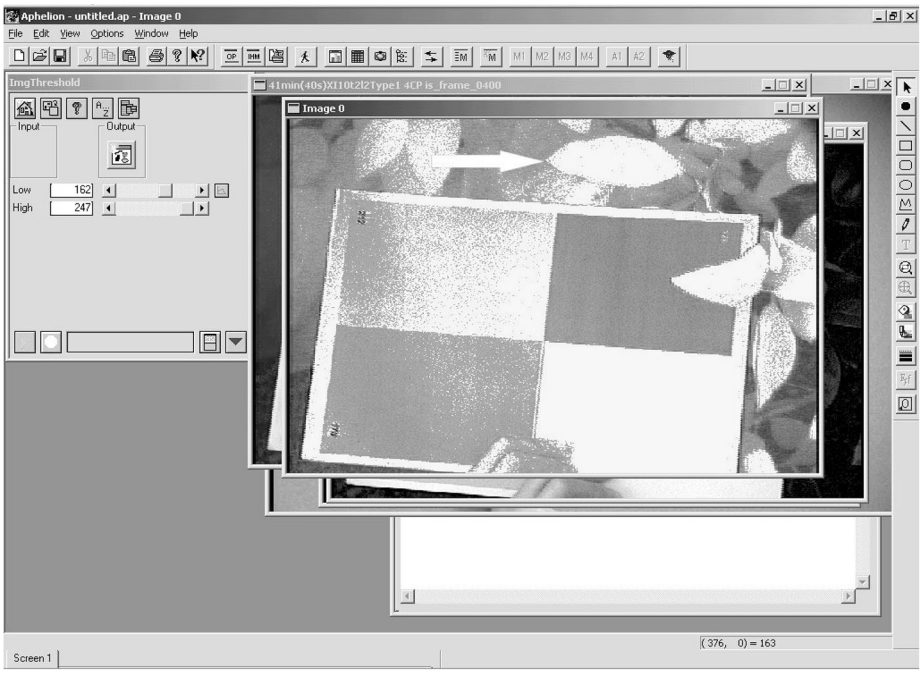

Figure 7. *Segmentation with ImgThreshold operator on a low contrast image. Arrow indicates the measured leaf object.*

http://www.ecology.kee.hu • ISSN 1589 1623

Similar to AphImgThreshold operator, Aphelion software contains several other threshold-based segmentation operators, that work specially (number of input parameters are shown in parenthesis):

- `ImgMomentThreshold (0),`
- `AphImgAdaptivePercentileThreshold (3),`
- `AphImgEntropyThreshold (0),`
- `AphImgHysteresisThreshold (4),`
- `AphImgMaximumContrastThreshold (1),`
- `AphImgMultiModalThreshold (6),`
- `AphImgExtremaThreshold (3)`

Operators generating Region Set

Each threshold-based operator has a pair with an additional function to generate Region Set. This means that in the first step the given operator returns a binary image, then in the second step, it groups the continuous pixels into objects to form a Region Set. These operators are named as threshold-based operators, following an …Obj ending.

To demonstrate Region Set generating operators function `AphImgHysteresisThresholdObj` operator is presented as an example. `AphImgHysteresisThreshold` operator applies two thresholds to the input image, outputting an image in which selected pixels are set to 1. A pixel is selected if its value is within the seed threshold range (first threshold), or if its value is within the hysteresis threshold range (second threshold), and there is a path of pixels connecting it to a seed valued pixel for which each pixel on the path has a value within the hysteresis threshold range. Requires the following parameters:

Inimg : input image,
Outimg : output image,

seedThresh : Seed threshold range (first threshold), constraint: SeedLoThresh value must be >= HysLoThresh value, and SeedHiThresh value must be <= HysHiThresh value,
SeedLoThresh : seed low threshold value,
SeedHiThresh : seed high threshold value,

hysThresh : Hysteresis threshold range (second threshold), constraint: HysLoThresh value must be <= SeedLoThresh value, and HysHiThresh value must be >= SeedHiThresh value,
HysLoThresh : hysteresis low threshold value,
HysHiThresh : hysteresis high threshold value.

http://www.ecology.kee.hu • ISSN 1589 1623

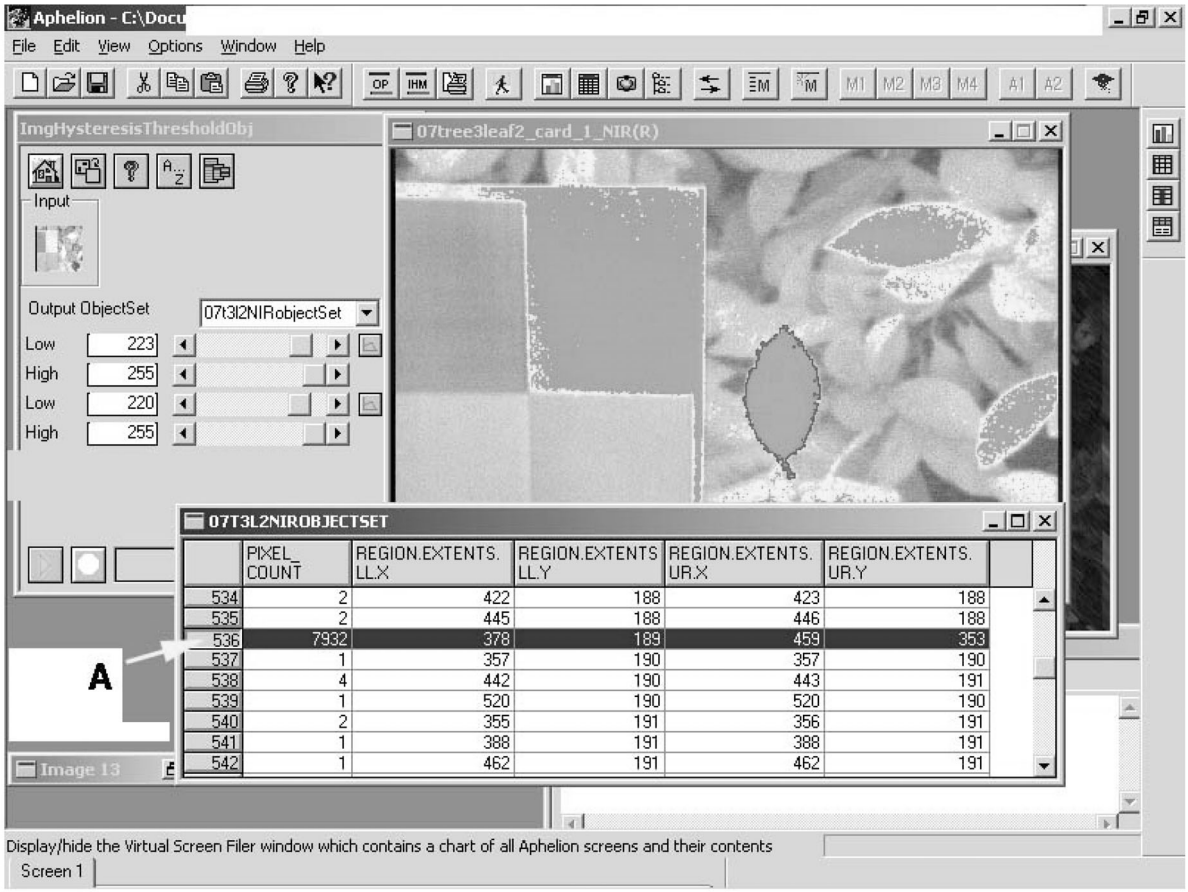

Figure 8. *A leaf object segmented by ImgHysteresisThresholdObj. 'A' indicates leaf object's properties.*

Figure 8 represents a screenshot result using AphImgHysteresisThresholdObj operator. Region Set objects' properties are described in the table shows the object's pixel number (PIXEL_COUNT), the bounding rectangle's lower left (REGION.EXTENTS.LL) and upper right (REGION.EXTENTS.UR) coordinates. Selected region's outline is red, unselected ones are marked yellow. Pink area indicates segmented pixels. Upper 'Low-High' values mean SeedLoThresh and SeedHiThresh values, HysLoThresh and HysHiThresh values locate under it as 'Low-High' values.

Region Set generating operators can extract segmented objects' outline, and convert into Region Of Interest (ROI), described below.

Region Of Interest (ROI)

It is practical to apply image processing methods not on the whole image, but select a part of the image and focus only that area. In Aphelion's terminology, this kind of area is called Region Of Interest (ROI), which can be defined either by Region Set or by upper left, and lower right coordinates of a rectangle-shaped ROI. Following a ROI definition, only the histogram of that area can be extracted, instead of the whole image's histogram. An adequately defined ROI can be used as a foreground after segmentation.

http://www.ecology.kee.hu • ISSN 1589 1623

Automatic segmentation of an image sequence

The practical, automatized usage of threshold-based operators is obstructed by two factors:

- Due to natural illumination conditions, the upper and lower threshold values are not constant, but change dynamically frame by frame. Optimal threshold values can be found only after several manual 'fine tuning' steps.
- Operators themselves require large computation capacity, and the analysis of several thousand frames was expected to require too long time.

It is necessary to automatize as many image analysis steps as possible considering the several thousand frames.

A reductive method emerged to solve this problem. Instead of calculating the exact contour of a leaf object with a definitely uneven outline, the object's inscribable rectangle was determined as defined as ROI. This rectangle has the feature that all of its enclosed pixels are inside of the object i. e. those are foreground pixels. Coordinate pairs of upper left and lower right corner can define a rectangle, and these coordinate values can automatically be passed to an operator as input parameters. All along the whole image analysis procedure, we had to take into account that as many as 100-300 images per leaf can be analyzed, and the objects' position relative to the frame often changed slightly. This effect might cause the ROI rectangle to contain background pixels. To avoid this, the ROI coordinates must have been chosen carefully.

Results and discussions

ROI corner coordinate definition

Using a videocamera instead of a still image camera allowed us to record a large amount of images i. e. visual data in short time. Frames were extracted from Type 2 AVI file into bitmap format still images at image analysis scheme step no. 3. This meant ~ 3-10 seconds video length, that corresponds around 100-300 images per leaf (29.97 images per second). Beside of the advantage of collecting large amount of visual information, this method also had a drawback in the form of object-shifting. Images were recorded under natural conditions and objects could not be tightened completely. Through 3-10 seconds per leaf recording duration object-shifting effect occurred in several cases. ROI corner coordinates must be defined a way to avoid the influence of shifting therefore ROI does not contain any background pixel.

http://www.ecology.kee.hu • ISSN 1589 1623

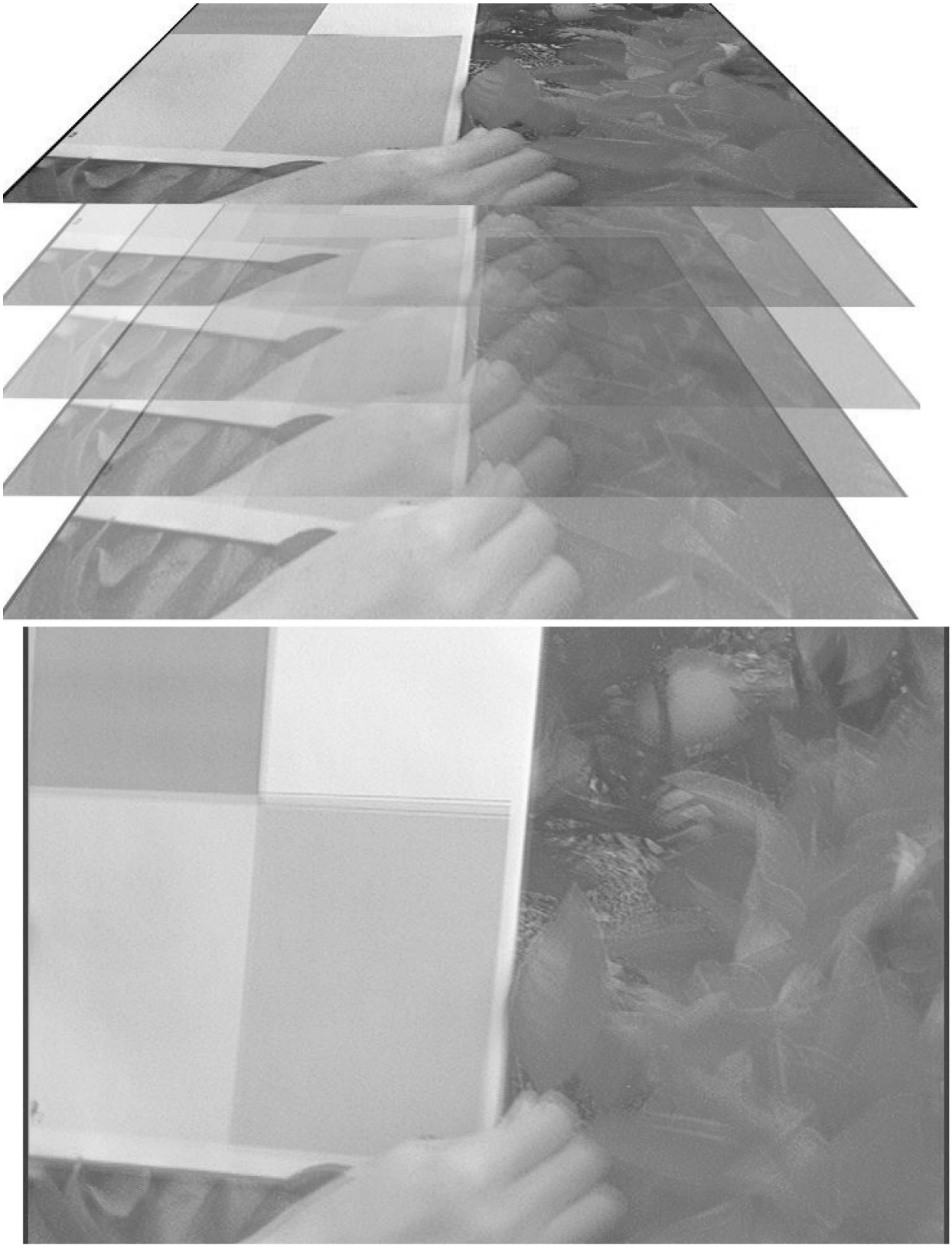

Figure 9. Merged lower image is composed by the upper 50% transparency 5 image layers. Blurred object outlines indicate the shifting phenomenon.

http://www.ecology.kee.hu • ISSN 1589 1623

In the case of a given leaf object every twentieth-fiftieth frame of the series was opened in a graphical software with multilayer capabilities (*Figure 9*). After the manual definition of ROI coordinates, it was ascertained that ROI contained only foreground pixels on all layers. In case of ROI contained background pixels on any layer, then ROI coordinate modification become necessary. In case of ROI did not contain background pixels on any layer, ROI coordinates were accepted. This procedure must have been performed only once per each leaf, and was found as an effective segmentation method.

Determine empirical density function by frequency table

Applying the AphImgBandHistogram, ROI pixels' intensity was extracted into a frequency table. SPSS software package was used to process data stored in frequency table. Further statistical analysis seemed to be difficult, because the type of objects' empirical density function was not uniform. Largely, objects' empirical density function showed normal (Gaussian) distribution (*Figure 10*).

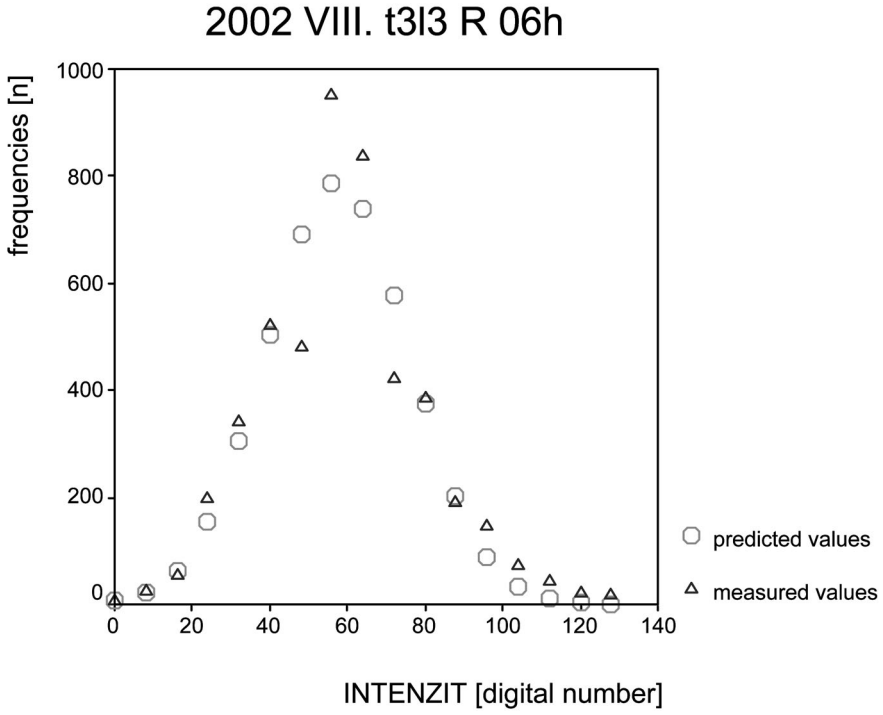

Figure 10. *Measured and predicted values of an object, whose reflectance shows normal distribution.* $\mu_{pred} = 57;\ \sigma_{pred} = 18;\ R^2 = 0{,}91$

Although normal distribution was found as a typical object density function, distinct type of functions also occurred. Both over- and under exposition caused 'shifted out' Gaussian curves from the perceptional range. Under exposition (*Figure 11*) evidently effected R and G bands where typically dark images were resulted due to the intensive light absorption. Over exposition (*Figure 12, 13*) effected the bright images of NIR band where light reflectance was intensive. Bimodal distribution also occurred. The reason of that phenomenon can be due to the non-flat surface of a leaf, and self-shading can occur: one part of the leaf seems shaded, another part seems sunlit (*Figure 14*).

http://www.ecology.kee.hu • ISSN 1589 1623

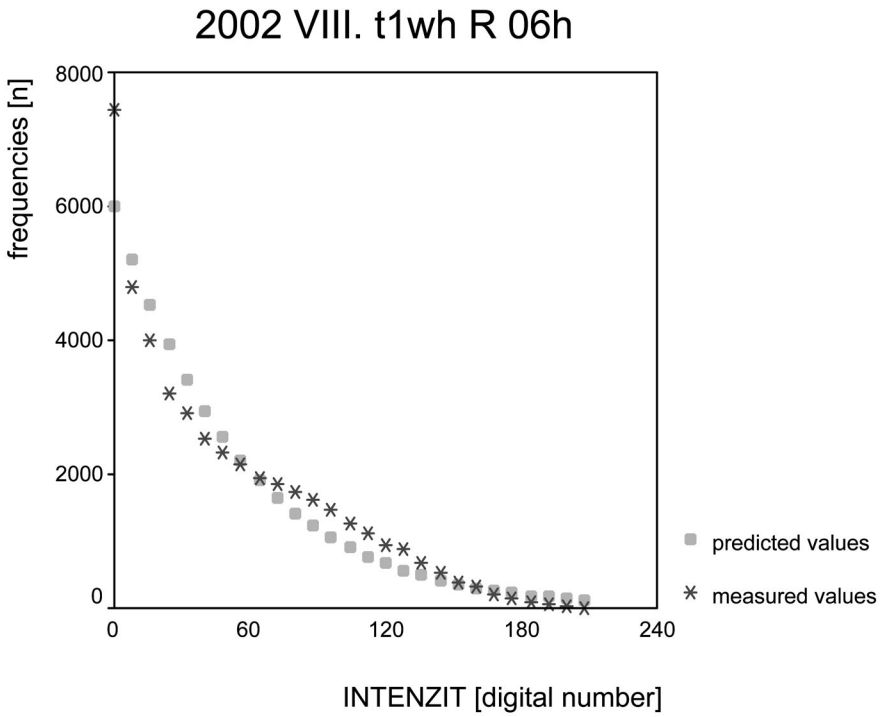

Figure 11. *Negatively shifted and truncated normal density function of an underexposed object's image.* $\mu_{pred} = -1255$ *(not interpretable);* $\sigma_{pred} = 268$ *(not interpretable);* $R^2 = 0{,}94$

Figure 12. *Image of an overexposed leaf object. White and gray areas indicate pixel intensity between 230 and 254, black areas indicate pixel intensity 255 or over.*

http://www.ecology.kee.hu • ISSN 1589 1623

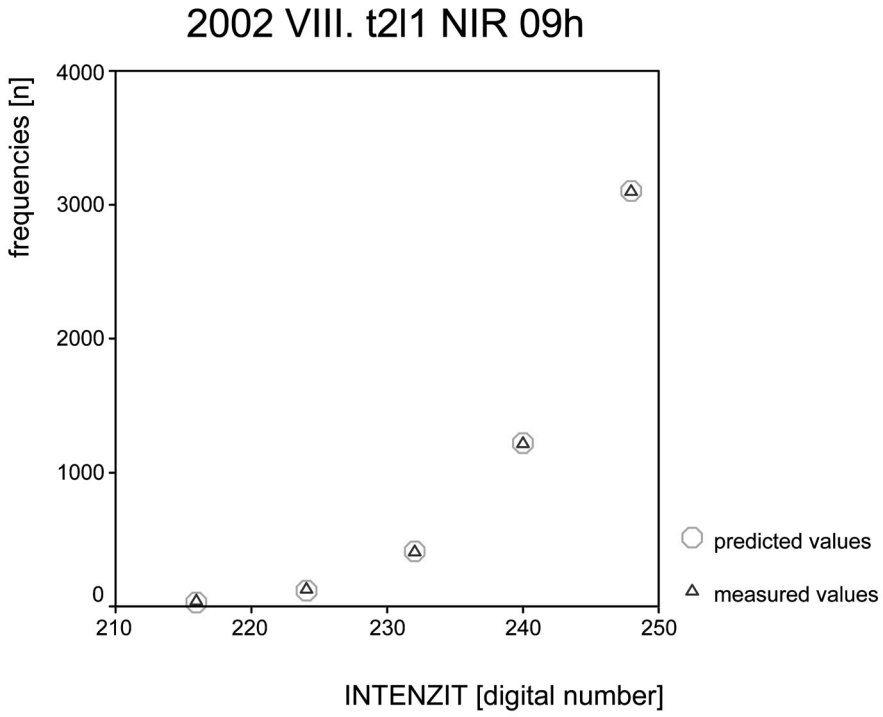

Figure 13. *Positively shifted and truncated normal density function of an overexposed object's image.* $\mu_{pred} = 298$ *(not interpretable);* $\sigma_{pred} = 21$; $R^2 = 0,99$

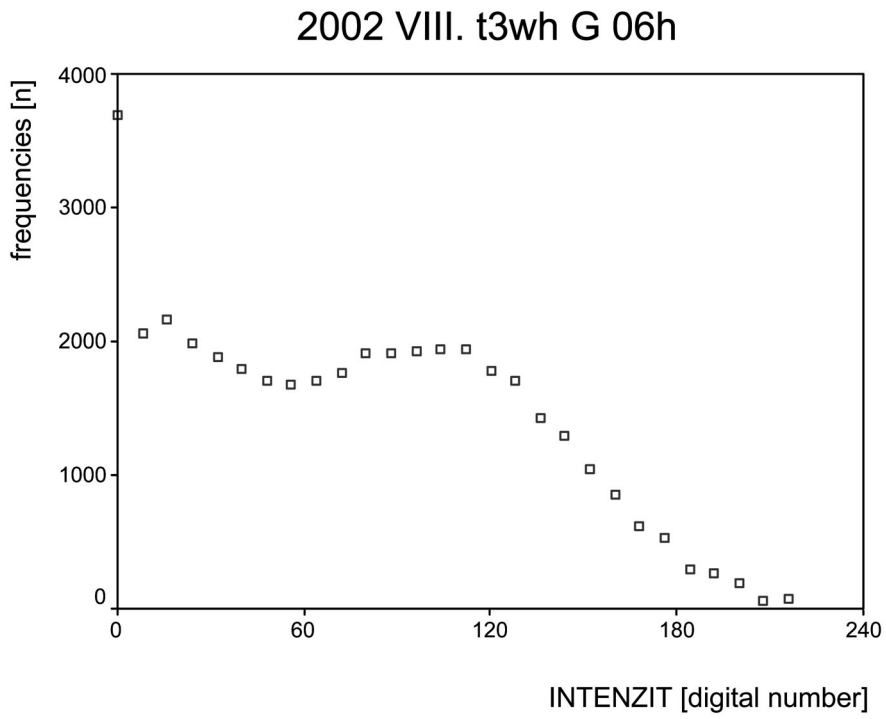

Figure 14. *Bimodal density function of a self-shaded leaf.*

http://www.ecology.kee.hu • ISSN 1589 1623

In case of data showing normal distribution the application of nonlinear regression (Eq. 1) was found to be practical, which resulted high R^2 value showing strong correlation.

This method was inadequate at cases showed non-normal distribution. Predicted

$$y = \frac{e^{-\frac{(x-\mu)^2}{2\sigma^2}}}{\sqrt{2\pi}\sigma} \qquad (1)$$

mean value result became smaller than zero in the case of underexposed images, and greater than 255 in the case of overexposed images. These results were not interpretable. Parameterization caused an other problem, because it could not be automatized. The estimated μ and σ values must have been provided manually one by one, separately for each objects (leaf or calibration plate), and this extremely slowed down the data analysis. The development of a uniform, algorithmizable statistical method was required to be able to analyze several thousand images, that showed several different distribution types. Weighted averaging (Eq. 2) was found to be a suitable method to solve the problems caused by self-shading, under- and over exposition. It ensures the μ and σ value results falling into the measurement range between 0 and 255, and did not require prerequisite, manual parameter estimation.

$$\overline{x}_a = \frac{\sum_{i=1}^{k} f_i x_i}{\sum_{i=1}^{k} f_i} \qquad (2)$$

As f_i values were discrete numerical values, so they are commutative and associative. This means that averaging (Eq. 3) can be used equivalently.

$$\overline{x}_a = \frac{\sum_{i=1}^{N} x_i}{N} \qquad (3)$$

Summary

In the frame of supporting precision agriculture fruit production system, the correlation between remotely sensed visual information and fruit tree physiological parameters were investigated. Significant amount of data was analyzed.

After successfully converting visual information into digital values, the objective became the characterization of a given object's (leaf, reference plate) reflectance. In the practice during statistical analysis of the visual information, technical and natural phenomena prevented the algorithmized, automatized application of normal curve fitting by nonlinear regression.

Experiments showed, that data-averaging method gives solution for practical statistical data interpretation problems caused by under-, over exposition, and self-shading due to a non-flat leaf surface.

http://www.ecology.kee.hu • ISSN 1589 1623

REFERENCES

[1] Vu, J.C.V., Yelenosky (1989): Non-structural carbohydrate concentrations in leaves of "Valencia" orange subjected to water deficits. – Environ. Expt. Bot. 29: 149-154.
[2] Kadoya, K. (1973): Studies on the translocation of photosynthates in Satsuma mandarin: Effects of water stress on the metabolism of sugars in the fruit. – J. Jpn. Soc. Hort. Sci. 42:210-214.
[3] Yakushiji, H. et al. (1996): Sugar accumulation enhanced by osmoregulation in Satsuma mandarin fruit. – J. Amer. Soc. Hort. Sci. 121:466-472.
[4] Elfving, D.C., Kaufmann M.R (1972): Diurnal and seasonal effects of environment on plant water relations and fruit diameter of citrus. – J. Amer. Soc. Hort. Sci. 97:566-570.
[5] Syvertsen, J.P. (1982): Minimum leaf water potential and stomatal closure in citrus leaves of different ages. – Ann. Botany 49:827-834.
[6] Norman S.M. et al. (1990): Abscisic acid accumulation and carotenoid and chlorophyll content in relation to water stress and leaf age of different types of citrus. – J. Agr. Food Chem. 38:1326-1334.
[7] Yakushiji, H., Morinaga K., Nonami H. (1998): Sugar Accumulation and Partitioning in Satsuma Mandarin Tree Tissues and Fruit in Response to Drought Stress. – J. Amer. Soc. Hort. Sci. 123(4), pp. 719-726.
[8] Láng, Z. et al. (2000): Precision farming alkalmazhatóságának kutatása a gyümölcstermesztésben. – MTA AMB Kutatási és Fejlesztési Tanácskozás, Gödöllő.
[9] Láng, Z., Molnár S. (2000): Image Processing Based Steering Control of a Plantation Tractor. – Proceedings AgEng Conference, Warwick, pp. 51-52.
[10] Láng, Z., Molnár S. (2000): Számítógépes képfeldolgozáson alapuló automatikus traktorirányítás modellkísérleteinek első eredményei. – MTA AMB Kutatási és Fejlesztési Tanácskozás, Gödöllő.
[11] Iwagaki, I. (1997): Citrus production in Japan: new trends in technology. – Food fertilizer & technology center, WWW-document, accessed on 05.01.1997. http://www.agnet.org/library/article/eb440.html
[12] Longshaw, T.G. (1974): Field spectroscopy for multispectral remote sensing: an analytical approach. –Applied Optics, 13: 1487-1493.
[13] Milton, E.J. (1987): Principles of field spectroscopy. – Int. J. Remote Sensing, 10 (6): 1041-1047.
[14] Palmer, J.M. (1982): Field Standards of Reflectance. – Photogrammetric Engineering and Remote Sensing. 48(10):1623-1625.
[15] Milton, E.J. (1989): On The Suitability of Kodak Neutral Test Cards as Reflectance Standards. – Int. J. Remote Sensing, 10 (6): 1041-1047.
[16] Kriston-Vizi, J., Umeda, M., Miyamoto, K., Ferenczy, A. (2003): Leaf Water Potential – Measurement Method Using Computer Image Analysis in Satsuma Mandarin. 2003 ASAE Annual International Meeting, Las Vegas, USA. Paper Number: 031050.
[17] Eastman Kodak Company (1999): How to use Koday Gray Cards. – Brochure Publication R-27.

http://www.ecology.kee.hu • ISSN 1589 1623